

See discussions, stats, and author profiles for this publication at: <https://www.researchgate.net/publication/231668162>

# Comparison of Techniques for Measuring the Electrical Double Layer Properties of Surfaces in Aqueous Solution: Hexadecyltrimethylammonium Bromide Self-Assembly Structures as a Mode...

ARTICLE in *LANGMUIR* · JULY 1995

Impact Factor: 4.46 · DOI: 10.1021/la00007a009

---

CITATIONS

61

---

READS

17

4 AUTHORS, INCLUDING:



**Calum J. Drummond**

RMIT University

190 PUBLICATIONS 7,002 CITATIONS

SEE PROFILE



**Peter J. Scales**

University of Melbourne

193 PUBLICATIONS 3,911 CITATIONS

SEE PROFILE

# Comparison of Techniques for Measuring the Electrical Double Layer Properties of Surfaces in Aqueous Solution: Hexadecyltrimethylammonium Bromide Self-Assembly Structures as a Model System<sup>†</sup>

Stephen B. Johnson,<sup>‡</sup> Calum J. Drummond,<sup>\*,§</sup> Peter J. Scales,<sup>\*,‡</sup> and Satoshi Nishimura<sup>⊥</sup>

*Advanced Mineral Products Research Centre, School of Chemistry, The University of Melbourne, Parkville, Victoria, 3052, Australia, CSIRO Division of Chemicals and Polymers, Private Bag 10, Rosebank MDC, Clayton, Victoria, 3169, Australia, and Government Industrial Research Institute, Kyushu, Agency of Industrial Science and Technology (MITI), Shuku-machi, Tosu, Saga 841, Japan*

Received December 5, 1994<sup>®</sup>

The effect of aqueous KBr concentration on the electrical double layer properties of two types of self-assembled hexadecyltrimethylammonium bromide (CTAB) surfaces has been investigated. A solvatochromic acid-base indicator has been used to determine the surface potential ( $\psi_0$ ) of CTAB micelles. Three different techniques have been employed to examine self-assembled CTAB bilayers adsorbed on amorphous silica surfaces. Flat plate streaming potentials ( $\zeta_s$  potentials), electrostatic potentials obtained from the electrophoretic mobility of relatively large colloid spheres ( $\zeta_e$  potentials), and diffuse layer potentials ( $\psi_d$ ) derived from the force versus separation curves for the interaction of a colloid sphere with a flat plate (measured with an atomic force microscope) have been analyzed.  $\zeta_s$  and  $\zeta_e$  potentials were found to be equivalent over a wide range of aqueous KBr concentration.  $\psi_d$  values in accord with  $\zeta_s$  and  $\zeta_e$  potentials were only derived in CTAB systems with a relatively low KBr concentration. At relatively high KBr concentrations ( $> 10^{-3}$  mol dm<sup>-3</sup>),  $\psi_d$  values were less than  $\zeta_s$  and  $\zeta_e$  potentials. This discrepancy has been attributed to the influence of surface roughness on the AFM force curve analysis. Micellar  $\psi_0$  values were larger than  $\zeta$  potentials. Analyses in terms of classical electrical double layer theory suggest that the degree of counterion dissociation from the surfactant headgroups ( $\alpha$ ) is markedly different for highly curved and planar surfaces;  $\alpha$  is in the range 0.05–0.11 for the adsorbed CTAB bilayers and in the range 0.29–0.43 for spherical CTAB micelles. Air/water surface tension curves have been employed to illustrate the effect that KBr has on minimum area per CTAB molecule at a planar interface and to provide values for the critical micelle concentration as a function of KBr concentration. CTAB micelles behave as Nernstian objects in KBr solution with the surfactant monomer acting as the potential determining ion. On the basis of this Nernstian behavior, a simple method has been employed to calculate the hydrophobic contribution to the free energy of CTAB micellization.

## Introduction

The placement of a surface with ionogenic groups in water may lead to the generation of an electrical double layer. The electrical double layer may make a significant contribution to aqueous solution processes such as interfacial ion adsorption, flocculation, and coagulation. As a means of characterizing the electrical double layer, surface associated electrostatic potentials are frequently measured, including flat plate streaming potentials ( $\zeta_s$  potentials), potentials obtained from the electrophoretic mobility of colloid spheres ( $\zeta_e$  potentials), and diffuse layer potentials ( $\psi_d$ ) derived by fitting DLVO theory to surface force versus separation curves.<sup>1</sup> One contentious issue is whether or not it can be assumed that these various electrostatic potentials are equivalent.

In this work, we take a model system and compare  $\zeta_s$  potentials,  $\zeta_e$  potentials, and  $\psi_d$  values derived from the force versus separation curves for the interaction of a colloid sphere with a flat plate (measured with an atomic force microscope). The model system is comprised of

hexadecyltrimethylammonium bromide (CTAB) bilayers adsorbed on amorphous silica surfaces in aqueous KBr solution. This system was selected because surface potentials ( $\psi_0$ ), diffuse layer potentials, and  $\zeta$  potentials are all likely to be equivalent since direct counterion binding will predominantly occur between the surfactant headgroups.

We also compare the surface potentials for highly curved CTAB micelles with the electrostatic potentials for the planar CTAB surface. Micellar surface potentials are obtained with a solvatochromic acid-base indicator technique.<sup>2</sup>

Air-water surface tension ( $\gamma_{LV}$ ) curves are employed to gauge the influence of salt on the packing of CTAB molecules at a planar surface. In addition, the  $\gamma_{LV}$  curves are used to obtain values for the critical micelle concentration (cmc) of CTAB as a function of KBr concentration. Reasons are given why we consider that  $\psi_0$  and cmc values can be used to estimate the hydrophobic contribution to the free energy of CTAB micellization.

## Experimental Section

**Materials.** Hexadecyltrimethylammonium bromide (CTAB) was obtained from Eastman Kodak (Rochester, NY). It was recrystallized twice from an acetone/ethanol mixture prior to use. Analytical grade KBr, KOH, and HBr (BDH Chemicals, Poole, England) were used without further purification. Water

\* Author to whom correspondence should be addressed.

<sup>†</sup> This work was presented at the 68th Meeting of the Colloid and Surface Chemistry Division of the American Chemical Society, Stanford University, June 21, 1994.

<sup>‡</sup> The University of Melbourne.

<sup>§</sup> Rosebank MDC.

<sup>⊥</sup> Agency of Industrial Science and Technology (MITI).

<sup>®</sup> Abstract published in *Advance ACS Abstracts*, May 15, 1995.

(1) Hunter, R. J. *Zeta Potential in Colloid Science*; Academic Press: London, 1981.

(2) Drummond, C. J.; Grieser, F.; Healy, T. W. *Faraday Discuss. Chem. Soc.* **1986**, *81*, 95.

used in this study was distilled before ultrapurification with charcoal and ion-exchange resins (Milli-Q: conductivity  $<1 \times 10^{-6} \Omega^{-1} \text{ cm}^{-1}$  at  $20^\circ \text{C}$ ).

Colloidal silica for use in electrophoresis and AFM studies was obtained in the form of microspheres with an average radius of  $6.5 \mu\text{m}$  (Polysciences, Warrington, PA). These were used as received. For the AFM investigations, silica microspheres were adhered to the end of v-shaped silicon nitride cantilevers (Digital Instruments, Santa Barbara, CA) with small quantities of molten epoxy resin (Epikote 1004, Shell). Cantilevers and attached silica colloids were treated with a mild water plasma prior to use. The AFM silica flat plate substrates were of two forms: suprasil grade fused silica (H.A. Groiss, Melbourne, Victoria, Australia) and a silicon wafer oxidized to a depth of  $1100 \text{ \AA}$  (Silica-Source Technology, Arizona). The silica flat plates used in streaming potential investigations were suprasil grade fused silica.

2,6-Diphenyl-4-(2,4,6-triphenyl-1-pyridino)phenoxide,  $\text{Et}(30)$ , was obtained from Aldrich Chemicals (Milwaukee, WI) and used without further purification. In order to aid aqueous dissolution,  $\text{Et}(30)$  was first mixed with a small volume of spectroscopic grade ethanol, before being added to surfactant solution.

**Procedures.** All experiments were performed at a temperature of  $32^\circ \text{C}$ , so as to remain above the CTAB Krafft temperature. The surface tension of the planar air/aqueous solution interface was determined using the du Noüy ring maximum force method.<sup>3</sup>

Flat plate streaming potential, colloid electrophoretic mobility, and colloid–flat plate AFM force measurements were conducted in the presence of  $1.5 \times 10^{-3} \text{ mol dm}^{-3}$  CTAB and varying amounts of KBr. In these experiments the pH was not adjusted.

The instrument and methodology involved in performing flat plate streaming potential measurements in the presence of adsorbed surfactant bilayers has been described elsewhere.<sup>4,5</sup> Solution pH and bulk conductivity were monitored using a Radiometer Model PHM 92 pH meter and a Philips Model PW 9526 digital conductivity meter, respectively. Electrophoresis measurements on colloidal silica spheres with adsorbed CTAB bilayers were performed on a Coulter Delsa 440 instrument.  $\zeta_e$  potentials were obtained from the electrophoretic mobility values by employing the Helmholtz–Smoluchowski equation.<sup>1</sup>

Direct measurements of the force of interaction between a silica colloid and a silica flat plate, both of which had an adsorbed CTAB bilayer, in aqueous solution were obtained with an atomic force microscope (Nanoscope III, Digital Instruments, Santa Barbara, CA).<sup>6–9</sup> The cantilever spring constants were experimentally determined by using the method of Senden and Ducker.<sup>10,11</sup> A detailed discussion of AFM force measurements in CTAB solutions is given elsewhere.<sup>9</sup>

For the two types of silica flat plates,  $5.0 \mu\text{m} \times 5.0 \mu\text{m}$  AFM images of the surface topography were obtained by employing v-shaped silicon nitride cantilevers with integrated square pyramidal tips in air with an applied load of  $\text{ca. } 10^{-10} \text{ N}$ .

$\text{Et}(30)$  was used to determine the CTAB micellar surface potentials. The procedure has been described in many previous studies.<sup>2,12,13</sup> Therefore only a brief account is given here.  $\text{Et}(30)$  possesses a prototropic moiety considered to reside pre-

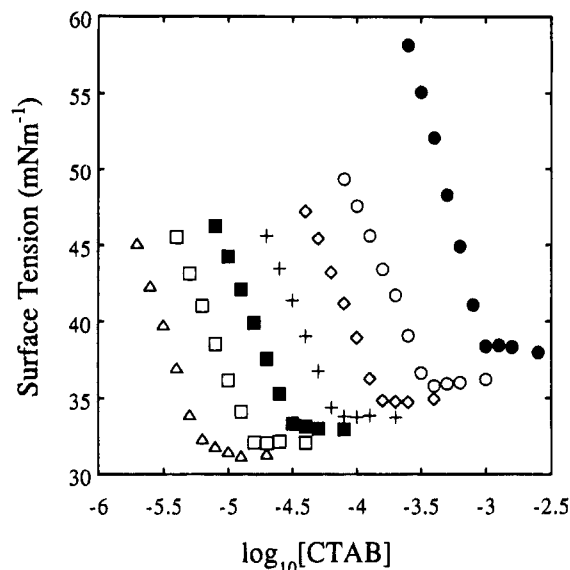


**Figure 1.** Air/aqueous solution interfacial tension,  $\gamma_{LV}$ , as a function of both CTAB and KBr concentrations;  $\bullet$ , 0 M KBr;  $\circ$ ,  $3.16 \times 10^{-3} \text{ M KBr}$ ;  $\diamond$ ,  $1.00 \times 10^{-2} \text{ M KBr}$ ;  $+$ ,  $3.16 \times 10^{-2} \text{ M KBr}$ ;  $\blacksquare$ , 0.100 M KBr;  $\square$ , 0.316 M KBr;  $\triangle$ , 1.00 M KBr.

dominantly in the mean plane of the cationic surfactant head-groups.<sup>2</sup> It was assumed that

$$\psi_0 = \left( \frac{2.303kT}{e} \right) (pK_a^\circ - pK_a^{\text{obs}}) \quad (1)$$

where  $pK_a^\circ$  and  $pK_a^{\text{obs}}$  are the intrinsic and observed  $pK_a$ s of the  $\text{Et}(30)$  probe molecule, respectively,  $k$  is the Boltzmann constant,  $e$  is the unit electronic charge, and  $T$  is the absolute temperature. The spectroscopic method for obtaining  $pK_a^\circ$  and  $pK_a^{\text{obs}}$  is given in the work of Drummond et al.<sup>2</sup> In the present work, the CTAB and  $\text{Et}(30)$  concentrations were  $5 \times 10^{-3}$  and  $5 \times 10^{-5} \text{ mol dm}^{-3}$ , respectively. The wavelength of the  $\text{Et}(30)$  solvatochromic absorption band maximum,  $\lambda_{\text{max}}$ , was used to determine the effective dielectric constant,  $\epsilon_{\text{eff}}$ , of the micellar interfacial microenvironment. System pH was monitored with a Radiometer Model PHM84 research pH meter. UV–visible spectroscopic absorption spectra were determined using both a Hewlett Packard Model 8451 diode array spectrophotometer and a Varian Cary Model 219 spectrophotometer.

## Results and Discussion

**Air/Aqueous Solution Surface Tension.** The variation of air/aqueous solution surface tension,  $\gamma_{LV}$ , as a function of both surfactant and electrolyte concentrations at  $32^\circ \text{C}$  is shown in Figure 1. The concentration of surfactant at the discontinuities is referred to as the critical micelle concentration (cmc). In the absence of added electrolyte, the experimental CTAB cmc of  $9.6 \times 10^{-4} \text{ mol dm}^{-3}$  compares well with literature values, which range between  $9.0 \times 10^{-4}$  and  $1.0 \times 10^{-3} \text{ mol dm}^{-3}$ .<sup>14</sup> The dependence of CTAB cmc values on ionic strength may be presented in the form of Corrin–Harkins equations.<sup>15</sup>

$$\log \text{cmc} = -0.76 \log(\text{cmc} + [\text{KBr}]) - 5.32 \quad (2)$$

$$[\text{KBr}] < 0.06 \text{ M}$$

$$\log \text{cmc} = -0.67 \log(\text{cmc} + [\text{KBr}]) - 5.18 \quad (3)$$

$$[\text{KBr}] \geq 0.06 \text{ M}$$

The existence of two linear Corrin–Harkins regimes has

(3) Furlong, D. N.; Freeman, P. A.; Metcalf, I. M.; White, L. R. *J. Chem. Soc., Faraday Trans. 1* **1983**, 79, 1701.

(4) Scales, P. J.; Grieser, F.; Healy, T. W.; White, L. R.; Chan, D. Y. *C. Langmuir* **1992**, 8, 965.

(5) Scales, P. J.; Grieser, F.; Healy, T. W.; Magid, L. J. *Langmuir* **1992**, 8, 277.

(6) Ducker, W. A.; Senden, T. J.; Pashley, R. M. *Nature (London)* **1991**, 353, 2.

(7) Ducker, W. A.; Senden, T. J.; Pashley, R. M. *Langmuir* **1992**, 8, 1831.

(8) Larson, I.; Drummond, C. J.; Chan, D. Y. C.; Grieser, F. *J. Am. Chem. Soc.* **1993**, 115, 11885.

(9) Drummond, C. J.; Senden, T. J. *Colloids Surf. A: Physicochem. Eng. Aspects* **1994**, 87, 217.

(10) Senden, T. J.; Ducker, W. A. *Langmuir* **1994**, 10, 1003.

(11) Drummond, C. J.; Senden, T. J. *Characterisation of the Materials Properties of Thin Film Cantilevers with the Atomic Force Microscope. Proceedings of INTERFACES II*; Materials Science Forum; Trans Tech Publications: Aedermannsdorf, Switzerland, 1994; in press.

(12) Drummond, C. J.; Grieser, F.; Healy, T. W. *Chem. Phys. Lett.* **1987**, 140, 493.

(13) Kibblewhite, J.; Drummond, C. J.; Grieser, F.; Healy, T. W. *J. Phys. Chem.* **1987**, 91, 4658. Murray, B. S.; Drummond, C. J.; Gale, L.; Grieser, F.; White, L. R. *Colloids Surf.* **1991**, 52, 287. Drummond, C. J.; Murray, B. S. *Prog. Colloid Polym. Sci.* **1992**, 88, 23.

(14) Mukerjee, P.; Mysels, K. L. *CMC of Aqueous Surfactant Solutions*; National Bureau of Standards; U.S. Government Printing Office: Washington, D.C., 1971.

(15) Corrin, M. L.; Harkins, W. D. *J. Am. Chem. Soc.* **1947**, 69, 683.

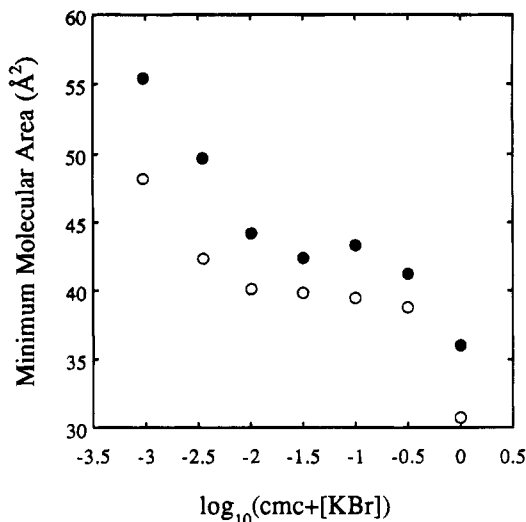


**Figure 2.** Minimum CTAB molecular areas at the air/aqueous solution interface (prior to the cmc),  $A_{\min}^{a/w}$  as a function of system ionic strength. Values of  $A_{\min}^{a/w}$  are calculated using both a quadratic (○) and linear (●) fit to surface tension data prior to the cmc.

been noted in several previous studies of simple cationic surfactant systems,<sup>16,17</sup> including CTAB/NaBr.<sup>18</sup> It has been suggested that it indicates a transition between spherical and rodlike micelles in solution. Recent static light scattering experiments with the CTAB/KBr system appear to support this explanation.<sup>19</sup>

Surfactant molecular packing densities at the air/aqueous solution interface were obtained by using the Gibbs adsorption treatment in the form due to Davies,<sup>20,21</sup>

$$\Gamma_{\max} = -\frac{1}{yRT} \left( \frac{d\gamma}{d \log[\text{CTAB}]} \right) \quad \text{and} \quad y = 1 + \left( \frac{[\text{CTAB}]}{[\text{CTAB}] + [\text{KBr}]} \right) \quad (4)$$

where  $\Gamma_{\max}$  is the maximum surface excess surfactant concentration and  $(d\gamma/d \log[\text{CTAB}])$  is the gradient of the relevant plot of surface tension versus the logarithm of surfactant concentration just prior to the cmc.

Corresponding minimum molecular areas at the air/aqueous solution interface,  $A_{\min}^{a/w}$ , were then calculated with use of the expression

$$A_{\min}^{a/w} = \frac{10^{16}}{N_A \Gamma_{\max}} \quad (\text{\AA}^2) \quad (5)$$

where  $N_A$  is the Avogadro number.

Two methods are currently used to determine the gradient of surface tension data at the cmc; a traditional linear fit to points over a range of ca. 10 mN m<sup>-1</sup> just below the cmc and a quadratic fit to data over a wider surface tension range prior to the cmc.<sup>22</sup> Minimum  $A_{\min}^{a/w}$  values calculated by both methods are shown for the CTAB/KBr system in Figure 2. Values obtained using the quadratic method are consistently lower than for the

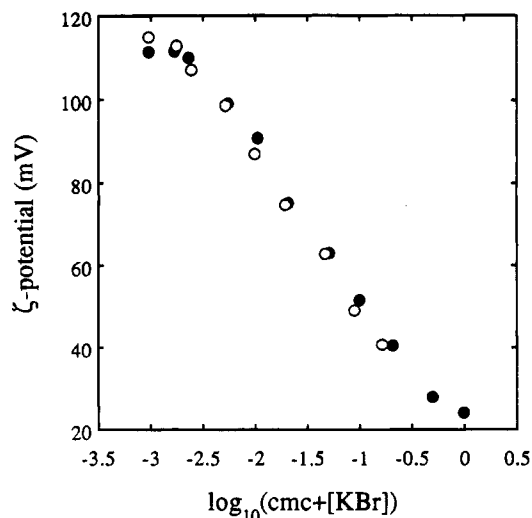


**Figure 3.** Variation of adsorbed CTAB bilayer  $\zeta$  potentials with solution ionic strength, as determined by flat plate streaming potential (○) and electrophoresis (●) techniques.

corresponding linear fit. The surface tension at the cmc,  $\gamma_{\min}$ , decreases as the KBr concentration increases (Figure 1). This is consistent with the decrease in  $A_{\min}^{a/w}$ .

**Adsorbed Surfactant Layers on Silica.** Figure 3 shows flat plate streaming potential and electrophoresis  $\zeta$  potentials as a function of ionic strength. In accordance with their electrokinetic basis, the two techniques provide similar  $\zeta$  potentials. The  $\zeta$  potentials for the CTAB/KBr system decrease as a function of increasing electrolyte concentration. A conventional electrical double layer treatment, with site-binding incorporated, has been used to interpret the  $\zeta$  potentials.<sup>4,5</sup>

The surface charge per unit area,  $\sigma_0$ , was determined by the number of dissociated surface sites, either as

$$\sigma_0 = e[\text{CTA}^+] \quad (6)$$

or, in the presence of a poorly neutralized background substrate, as

$$\sigma_0 = 2e[\text{CTA}^+] - \sigma_{\text{back}} \quad (7)$$

where  $\sigma_{\text{back}}$  is the charge of the background silica substrate.

The number of surfactant units within each layer,  $N_x$ , was given by

$$N_x = [\text{CTA}^+] + [\text{CTA}^+\text{Br}^-] \quad (8)$$

The degree of bilayer dissociation,  $\alpha$ , was then calculated with

$$\alpha = [\text{CTA}^+]/N_x \quad (9)$$

A Gouy–Chapman approach to the planar electrical double layer interface was taken so that

$$\sigma_0 + \sigma_d = 0 \quad (10)$$

where  $\sigma_d$  is the diffuse layer charge.

Double layer potentials and charge densities were related through the notion of an interfacial capacitance with

$$\psi_0 - \psi_d = \sigma_0/C_1 \quad (11)$$

where  $\psi_0$  is the surface potential,  $\psi_d$  is the diffuse layer potential, and  $C_1$  is the interfacial capacitance.

(16) Ikeda, S.; Ozeki, S.; Tsunoda, M. *J. Colloid Interface Sci.* **1980**, *73*, 27.

(17) Ozeki, S.; Ikeda, S. *J. Colloid Interface Sci.* **1982**, *87*, 424.

(18) Okuda, H.; Imae, T.; Ikeda, S. *Colloids Surf.* **1987**, *27*, 187.

(19) Imae, T.; Kamiya, R.; Ikeda, S. *J. Colloid Interface Sci.* **1985**, *108*, 215.

(20) Matijevic, E.; Pethica, B. A. *Trans. Faraday Soc.* **1958**, *54*, 1382.

(21) Rosen, M. J. *Surfactants and Interfacial Phenomena*; Wiley-Interscience: New York, 1978.

(22) Simister, E. A.; Thomas, R. K.; Penfold, J.; Aveyard, R.; Binks, B. P.; Cooper, P.; Fletcher, P. D. I.; Lu, J. R.; Sokolowski, A. *J. Phys. Chem.* **1992**, *96*, 1383.

The diffuse layer charge was calculated by using the relationship

$$\sigma_d = -[8n_0\epsilon\epsilon_0 kT]^{1/2} \sinh\left(\frac{ze\psi_d}{2kT}\right) \quad (12)$$

where  $n_0$  is the number concentration of ions in the bulk solution,  $\epsilon$  is the dielectric constant of the bulk medium, and  $\epsilon_0$  is the permittivity of free space.

Values of  $n_0$  were determined by using two approximations,

$$n_0 \approx [\text{KBr}] + \text{cmc} \quad \text{low approximation} \quad (13)$$

$$n_0 \approx [\text{KBr}] + \alpha([\text{CTA}^+\text{Br}^-] - \text{cmc}) + \text{cmc} \quad \text{high approximation} \quad (14)$$

The actual value of  $n_0$  should lie between the bounds set by eqs 13 and 14.

Diffuse layer potentials,  $\psi_d$ , were estimated from flat plate streaming potential studies, assuming near equivalence of the diffuse layer plane and the electrokinetic plane of shear.<sup>1,23,24</sup> Surfactant surface sites,  $N_s$ , were incorporated by assuming that the minimum molecular areas obtained from surface tension studies at the air/aqueous solution interface could be employed. In effect we have assumed that the packing of an adsorbed monolayer of CTAB at the hydrophobic air/water interface will be equivalent to that of an adsorbed monolayer of CTAB at the hydrophobic hexadecyl chain/water interface. This is likely to be the case if there is little interdigitation of the hexadecyl chains in the adsorbed CTAB bilayer on silica. We used the  $A_{\text{min}}^{a/w}$  values obtained from the quadratic fit to the surface tension curves, but using the other set of values provides almost identical results. The background silica charge,  $\sigma_{\text{back}}$ , was estimated from previous streaming potential studies on similar silica substrates.<sup>4</sup> Values of  $C_1$  were assumed to lie between 200 and 1000  $\mu\text{F cm}^{-2}$  (i.e.  $\psi_0 \approx \psi_d$ ).<sup>5</sup> Equations 6–14 were solved for both limits of  $n_0$  and  $C_1$  by using a series of linked interval halving methods.<sup>4</sup>

Degrees of CTAB outer layer dissociation,  $\alpha$ , calculated both with and without incorporation of a residual silica background charge, are shown in Figure 4. Whether upper or lower limits of  $n_0$  were incorporated into the modeling scheme was found to be of little significance to the values of  $\alpha$  obtained. Calculated degrees of CTAB outer layer dissociation were also found to be relatively independent of the electrical double layer capacitance that was utilized. The degree of dissociation rises gradually with added electrolyte. The extent of this increase is found to be slightly greater when background silica substrate charge is neglected.

The influence of using counterion activities instead of concentrations was also assessed. In this semithermodynamic approach to bilayer modeling, values of  $n_0$  were substituted by solution activities in eq 12. Activities were calculated by using the expression

$$A = \gamma_i n_0 \quad (15)$$

The activity coefficient,  $\gamma_i$ , was determined by using the

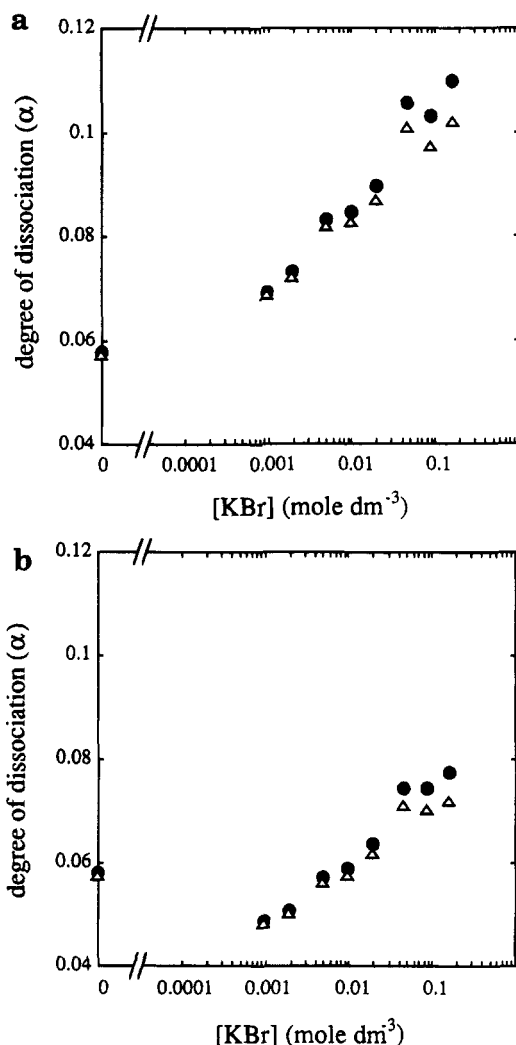


**Figure 4.** Calculated degrees of CTAB bilayer dissociation,  $\alpha$ , as a function of KBr concentration. Values of  $\alpha$  are determined both (a, top) without and (b, bottom) with incorporation of residual silica background charge, using concentration ( $\bullet$ ) and activity ( $\Delta$ ) data.

extended Debye–Hückel limiting law<sup>25</sup>

$$\ln \gamma_i = \frac{-2.303A_m(n_0)^{1/2}}{1 + B_m a(n_0)^{1/2}} \quad (16)$$

where  $a$  is the mean distance of closest approach of the bromide ion in solution, and  $A_m$  and  $B_m$  are constants (0.52 and 0.33, respectively, at 32 °C).

Figure 4 shows degrees of CTAB outer layer dissociation when activities are used in the treatment. Values of  $\alpha$  are found to deviate only slightly from those calculated with  $n_0$ . Under these conditions, treating concentrations and activities as equivalent would appear to be acceptable.

The  $\alpha$  values for the CTAB bilayer on silica can be compared with the values for other alkyl quaternary ammonium bromide surfactant bilayer systems, including didodecyltrimethylammonium bromide (DDDAB), ditetradecyltrimethylammonium bromide (DTDAB), dihexadecyltrimethylammonium bromide (DHDAB), and dioctadecyltrimethylammonium bromide (DODAB) systems. The  $\alpha$  values of Figure 4 are in reasonable accord with  $\alpha$  values calculated for DDDAB and DHDAB vesicles by utilizing solvatochromic acid–base indicator measured

(23) Stigter, D. *J. Phys. Chem.* **1964**, *68*, 3600.

(24) Carrol, B. J.; Haydon, D. A. *J. Chem. Soc., Faraday Trans. 1* **1975**, *71*, 361.

(25) Robinson, R. A.; Stokes, R. H. *Electrolyte Solutions*, 2nd ed.; Butterworths: London, 1959. Wilk, K. A.; Burczyk, B.; Kubica, H. *Colloids Surf.* **1990**, *50*, 363.

$\psi_0$  values,<sup>26</sup> DDDAB and DTDAB vesicles  $\zeta_0$  potentials,<sup>27</sup> DDDAB and DHDAB bilayers adsorbed on mica  $\zeta_s$  potentials,<sup>28,29</sup> DODAB deposited on mica with the Langmuir–Blodgett technique derived from surface force apparatus (SFA)  $\psi_d$  values,<sup>30</sup> DHDAB and CTAB adsorbed on mica derived from SFA  $\psi_d$  values,<sup>31,32</sup> and thin liquid CTAB soap films where light scattering was utilized to derive  $\psi_d$  values.<sup>33</sup> At this stage, two SFA studies<sup>34,35</sup> where CTAB bilayers were adsorbed on mica appear anomalous, as the derived  $\psi_d$  and  $\alpha$  values are much higher than those found for other similar planar surfaces.<sup>9</sup> We have plans to check the results for the CTAB/mica system with streaming potential measurements.

By assuming that a complete surfactant bilayer has adsorbed to the silica substrate, the outer CTAB monolayer dissociation constant,  $K_{\text{diss}}$ , can be calculated



$$K_{\text{diss}} = \frac{[\text{CTA}^+][\text{Br}^-]_s}{[\text{CTA}^+\text{Br}^-]} \quad (17)$$

where  $[\text{CTA}^+]$  and  $[\text{CTA}^+\text{Br}^-]$  are the concentrations of ionized and neutralized surfactant monomers, respectively, and  $[\text{Br}^-]_s$  is the surface concentration of bromide ions

$$[\text{Br}^-]_s = [\text{Br}^-]_b \exp(e\psi_0/kT) \quad (18)$$

where  $[\text{Br}^-]_b$  is the bulk concentration of bromide ions. It follows that

$$\frac{[\text{CTA}^+]}{[\text{CTA}^+\text{Br}^-]} = \frac{\alpha}{1 - \alpha} \quad (19)$$

and combining eqs 16–19 leads to the expression

$$K_{\text{diss}} = \frac{\alpha}{1 - \alpha} [\text{Br}^-]_b \exp\left(\frac{e\psi_0}{kT}\right) \quad (20)$$

Values of  $pK_{\text{diss}}$  determined assuming both poor and complete background substrate neutralization are shown in Figure 5. There is a gradual decrease of  $pK_{\text{diss}}$  as the ionic strength increases. The magnitude of the decrease is slightly greater when background substrate charge is neglected. The inclusion of counterion activities has no significant effect on the  $pK_{\text{diss}}$  behavior.

Fuoss and Kraus have reported thermodynamic  $pK_{\text{diss}}$  values for tetrabutylammonium bromide (TBAB) in 1,4-dioxane/water (D/W) mixtures.<sup>36</sup> The  $pK_{\text{diss}}$  values of TBAB in water, a 50 wt % D/W mixture ( $\epsilon = 35.9$ ), and a 70 wt % D/W mixture ( $\epsilon = 19.1$ ) are  $-0.21$ ,  $0.66$ , and

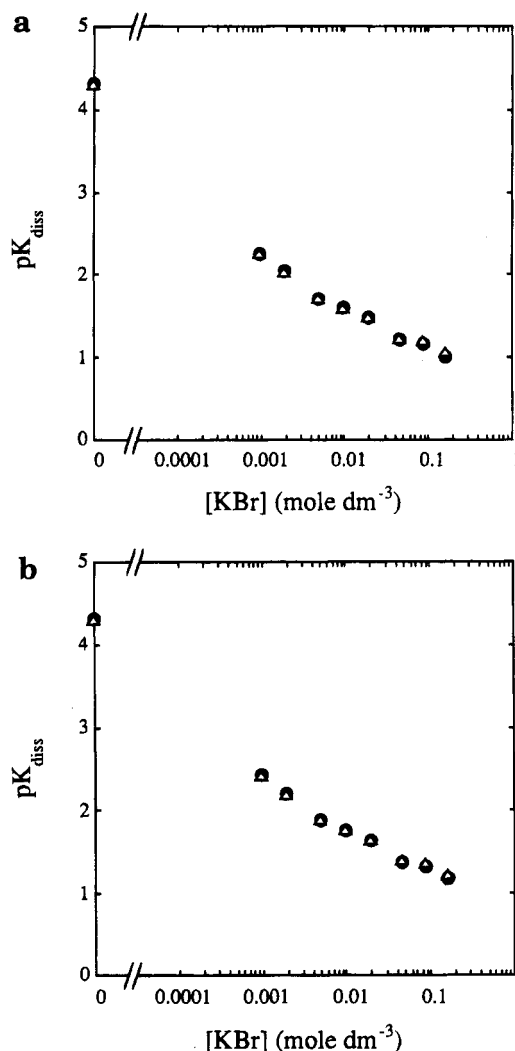


**Figure 5.** Calculated values of  $pK_{\text{diss}}$  for the CTAB bilayer system as a function of KBr concentration. Values of  $pK_{\text{diss}}$  are determined both (a, top) without and (b, bottom) with incorporation of residual silica background charge, using concentration (●) and activity (△) data.

$2.01$ , respectively. Therefore the  $pK_{\text{diss}}$  values for the CTAB planar interfaces have the expected order.

The nonconstant nature of the  $pK_{\text{diss}}$  values for the planar CTAB interfaces in KBr solutions is intriguing. At this stage, we cannot unequivocally explain this result. At least three explanations are possible. First, electrolyte induced changes in the solvent properties of the interfacial microenvironment (including steric hindrance) may be responsible. Second, there may be a small error associated with using  $A_{\text{min}}^{a/w}$  to estimate the surface group density. Third, the apparent change in  $pK_{\text{diss}}$  may be an artifact of treating the surface charges as residing in a plane when the actual CTAB interface will have molecular protrusion and a distribution (transverse displacement) of surface charge.<sup>37,38</sup>

Figure 6 shows a force/radius ( $F/R$ ) versus intersurface separation plot obtained with the AFM sphere–flat plate arrangement. On the example shown, the presence of a CTAB bilayer on both silica surfaces is clearly indicated by the dual “step-ins” just prior to the onset of the exponential diffuse layer potential decay (see inset). The step-ins were not always present; it was more usual to observe “hard wall” surface contact without any measurable change in intersurface separation as the applied pressure was increased. Each step-in was  $\text{ca. } 3.5 \pm 0.4$

(26) Drummond, C. J.; Grieser, F.; Healy, T. W. *J. Phys. Chem.* **1988**, *92*, 2604.

(27) Kaneko, Y.; Miller, D. D.; Evans, D. F. *J. Solution Chem.* **1990**, *19*, 457.

(28) Scales, P. J.; Grieser, F.; Healy, T. W.; Magid, L. J. *Langmuir* **1992**, *8*, 277.

(29) Nishimura, S. Unpublished data.

(30) Marra, J. *J. Phys. Chem.* **1986**, *90*, 2145.

(31) Pashley, R. M.; Israelachvili, J. N. *Colloids Surf.* **1981**, *2*, 169.

(32) Pashley, R. M.; McGuiggan, P. M.; Ninham, B. W.; Brady, J.; Evans, D. F. *J. Phys. Chem.* **1986**, *90*, 1637.

(33) Donners, W. A. B.; Rijnhout, J. B.; Vrij, A. *J. Colloid Interface Sci.* **1977**, *61*, 249.

(34) Pashley, R. M.; McGuiggan, P. M.; Horn, R. G.; Ninham, B. W. *J. Colloid Interface Sci.* **1988**, *126*, 569.

(35) Kékecheff, P.; Christenson, H. K.; Ninham, B. W. *Colloids Surf.* **1989**, *40*, 31.

(36) Fuoss, R. M.; Kraus, C. A. *J. Am. Chem. Soc.* **1957**, *79*, 3304.

(37) Cevc, G.; Svetina, S.; Bostjan, Z. *J. Phys. Chem.* **1981**, *85*, 1762.

(38) Bohmer, M.; Koopal, L. K. *Langmuir* **1992**, *8*, 1594.

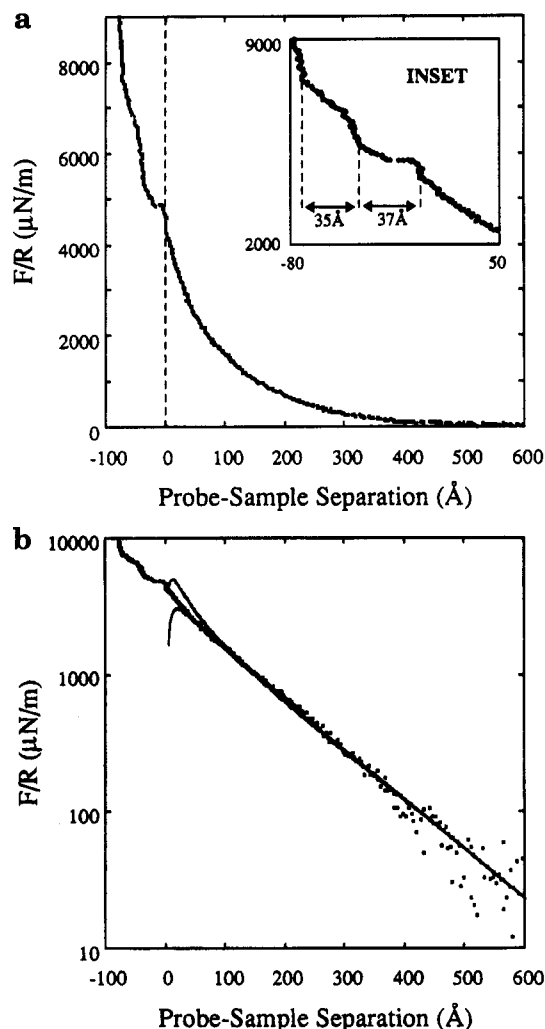


**Figure 6.** (a, top) Force/radius versus intersurface separation for a CTAB bilayer adsorbed on a silica colloid interacting with a CTAB bilayer adsorbed on a flat oxidized silicon wafer. The CTAB concentration in solution is  $1.5 \times 10^{-3}$  M. The presence of a CTAB bilayer on both surfaces is indicated by the dual step-ins prior to the onset of exponential electrical double layer decay (see inset). (b, bottom) Force/radius (logarithmic scale) versus intersurface separation for the same CTAB adsorbed bilayer system as a. Upper and lower line plots correspond to constant charge and constant potential DLVO fits, respectively.  $\psi_d = 90$  mV;  $A_H = 5 \times 10^{-21}$  J.

nm. This can be compared with other measurements of the thickness of an adsorbed CTAB bilayer:  $3.4 \pm 0.2$  nm from neutron reflection<sup>39</sup> and  $3.3 \pm 0.2$  nm from SFA<sup>31,34,35</sup> measurements.

Diffuse electrical double layer potentials,  $\psi_d$ , were determined by fitting experimental  $F/R$  curves to the standard DLVO treatment<sup>40,41</sup> for the interaction between two identical flat plates. The silica sphere is sufficiently large so that the Derjaguin approximation<sup>42,43</sup> can be used to link the sphere–flat plate interaction force,  $F_{sp}$ , to the interaction energy per unit area between flat plates,  $V_{pp}$ ,

$$V_{pp} = F_{sp}/2\pi R \quad (21)$$

where  $R$  is the radius of the silica sphere. It is assumed

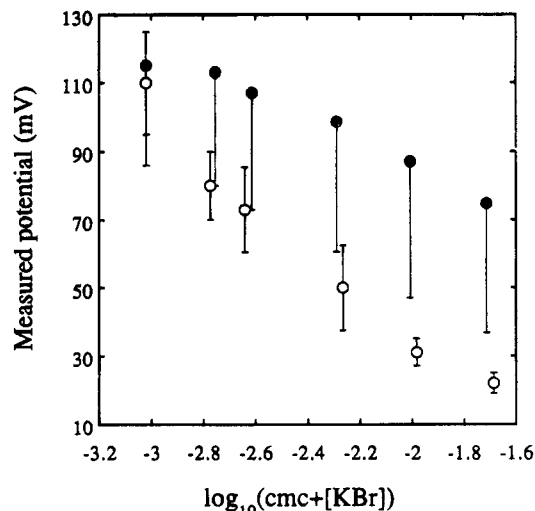


**Figure 7.** Diffuse layer potentials (○) as a function of system ionic strength determined from atomic force microscopy force-separation curves for a silica slide/CTAB bilayer/aqueous KBr solution/CTAB bilayer/silica colloid system. Electrokinetic  $\zeta$  potential data (●) are also plotted for comparison. The vertical bars on the electrokinetic data are discussed in the text.

that

$$F_{sp} = F_{vdw} + F_{edl} \quad (22)$$

$F_{vdw}$  is the van der Waals force

$$F_{vdw} = -A_H R/6H^2 \quad (23)$$

where  $A_H$  is the nonretarded Hamaker constant set at  $5.0 \times 10^{-21}$  J<sup>44</sup> and  $H$  is the intersurface separation.  $F_{edl}$  is the electrical double layer force which was calculated by using the nonlinearized Poisson–Boltzmann equation at both constant charge and constant potential boundary conditions.<sup>45</sup> The location of the diffuse layer plane of charge and the plane of origin of the van der Waals interaction were set at the apparent CTAB bilayer–bilayer contact position (at the outer extent of the bilayer step-ins when they were present). The value for  $\psi_d$  was taken as that which gave the best fit of DLVO theory to the experimental force curves. The calculated  $\psi_d$  values were independent of whether or not step-ins were present.

CTAB diffuse layer potentials derived from the AFM force-separation curves are shown as a function of ionic strength in Figures 7 and 8. Figures 7 and 8 refer to suprasil silica and oxidized silicon wafer flat plates, respectively.  $\zeta_s$  potentials are included on the figures for comparison. The vertical bars on the electrokinetic data are discussed below. At KBr concentrations greater than  $ca. 10^{-3}$  mol dm<sup>-3</sup> KBr, potentials estimated from AFM studies are considerably lower than the  $\zeta_s$  potentials. The  $\psi_d$  value for the CTAB system with the oxidized silicon wafer as the flat plate and no KBr is in quantitative agreement with the result from an earlier study using a similar sphere–flat plate setup.<sup>9</sup>

The location of the average plane of charge in relation to the hard wall contact position is a very important consideration. Accurate determination of  $\psi_d$  values from AFM force curves relies upon surfaces contacting in the

(41) Verwey, E. J. W.; Overbeek, J. T. G. *The Theory of the Stability of Lyophobic Colloids*; Elsevier: Amsterdam, 1948.

(42) Derjaguin, B. V. *Kolloid Z.* **1934**, 69, 155.

(43) White, L. R. *J. Colloid Interface Sci.* **1983**, 95, 286.

(44) Hough, D. B.; White, L. R. *Adv. Colloid Interface Sci.* **1980**, 14, 3.

(45) Chan, D. Y. C.; Pashley, R. M.; White, L. R. *J. Colloid Interface Sci.* **1980**, 77, 283.

(39) McDermott, D. C.; McCarney, J.; Thomas, R. K.; Rennie, A. R. *J. Colloid Interface Sci.* **1994**, 162, 304.

(40) Derjaguin, B. V.; Landau, L. *Acta Physicochim. URSS* **1941**, 14, 633.

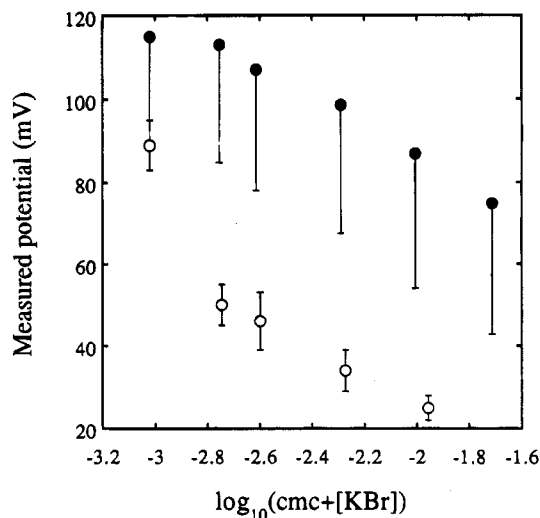


**Figure 8.** Diffuse layer potentials (○) as a function of system ionic strength determined from atomic force microscopy force-separation curves for an oxidized silicon wafer/CTAB bilayer/aqueous KBr solution/CTAB bilayer/silica colloid system. Electrokinetic  $\zeta$  potential data (●) are also plotted for comparison. The vertical bars on the electrokinetic data are discussed in the text.

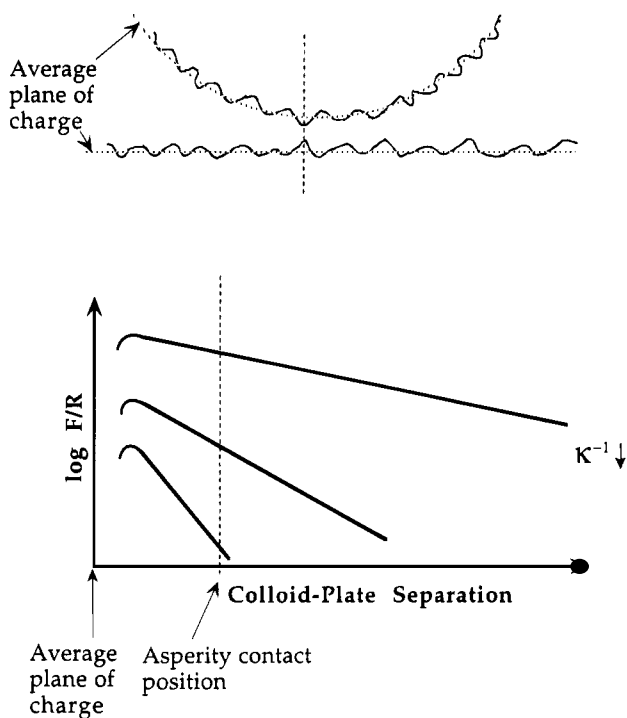


**Figure 9.** Effect of surface roughness on atomic force microscopy force curve analysis. The magnitude of the errors introduced by random asperity contact is shown to increase as the solution ionic strength rises, due to the more rapid electrical double layer decay.

average plane of charge. In general, however, both the colloid sphere and flat plate surfaces possess a random distribution of asperity heights. Should contact occur at such a site, rather than in the average plane of charge, the derived  $\psi_d$  value will be an underestimate. This becomes a significant problem as the extent of the surface force approaches the magnitude of the surface roughness. Consequently, for charged surfaces, roughness becomes more of a problem as the ionic strength is increased. The problem is displayed schematically in Figure 9, where it is shown how assuming that the asperity contact position is the origin of the force of interaction can be misleading.

AFM images ( $5\ \mu\text{m} \times 5\ \mu\text{m}$ ) showed that the surfaces of the oxidized silicon wafer and silica slide had root mean

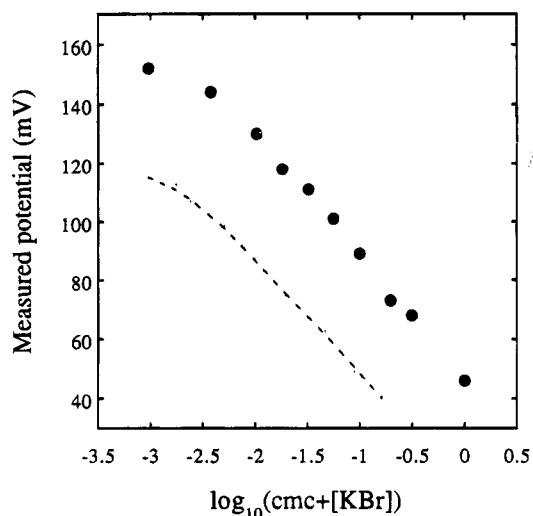


**Figure 10.** CTAB micellar surface potentials, determined by the solvatochromic acid-base indicator technique, as a function of solution ionic strength. Electrokinetic data (- -) are given for the purpose of comparison.

square (rms) roughness of 0.8 nm and 1.5 nm, respectively. The maximum height of any feature on the oxidized silicon wafer and silica slide were *ca.* 10 nm and *ca.* 50 nm, respectively. The rms roughness of the silica colloids has been reported as 1.5 nm.<sup>7</sup> We examined the effect of shifting the diffuse layer charge plane and van der Waals' plane to a negative surface contact separation, corresponding to the combined rms roughness of both the colloid and flat plate surfaces. A similar procedure has been followed by Smith et al. in analyzing their SFA  $F/R$  versus  $H$  curves for thin platinum films on mica.<sup>46</sup> The bars displayed in Figures 7 and 8 illustrate how following this analysis procedure results in an apparent  $\psi_d$  value that is significantly less than the  $\zeta_s$  potential. Experimental  $\psi_d$  values are only found to fall within the bars at low ionic strengths. Interestingly, the agreement between  $\zeta$  potential and AFM derived  $\psi_d$  is worse for the oxidized silicon wafer while this surface has the smallest rms roughness. This re-emphasizes the difficulties in attempting to realistically model random surface roughness effects.<sup>9</sup>

**Micelles.** CTAB micellar surface potentials,  $\psi_0$ , determined by the solvatochromic acid-base indicator technique, are shown as a function of solution ionic strength in Figure 10. There is a reduction in micellar surface potential as the ionic strength increases. The  $\psi_0$  value in the CTAB system without added electrolyte (156 mV) is greater than the value quoted elsewhere<sup>2</sup> (141 mV) due to the different electrolyte effect of solutions with  $5 \times 10^{-3}$  and  $5 \times 10^{-2}$  mol dm<sup>-3</sup> CTAB. Micellar  $\psi_0$  values are significantly greater than the  $\zeta$  potentials for effectively planar surfactant surfaces. This is consistent with the results of a recent neutron reflection study.<sup>47</sup>

The complex dynamic surfactant self-assembly system was greatly simplified by modeling the CTAB micelles as monodisperse impenetrable spheres of uniform charge density. It was assumed that the relationship between the micellar surface charge density,  $\sigma_0$ , and the electrostatic surface potential may be given by the unmodified nonlinearized Poisson-Boltzmann equation in spherical symmetry.<sup>12</sup>

(46) Smith, C. P.; Maeda, M.; Atanasoska, L.; White, H. S.; McClure, D. J. *J. Phys. Chem.* **1988**, 92, 199.

(47) Lu, J. R.; Simister, E. A.; Thomas, R. K.; Penfold, J. *J. Phys. Chem.* **1993**, 97, 13907.



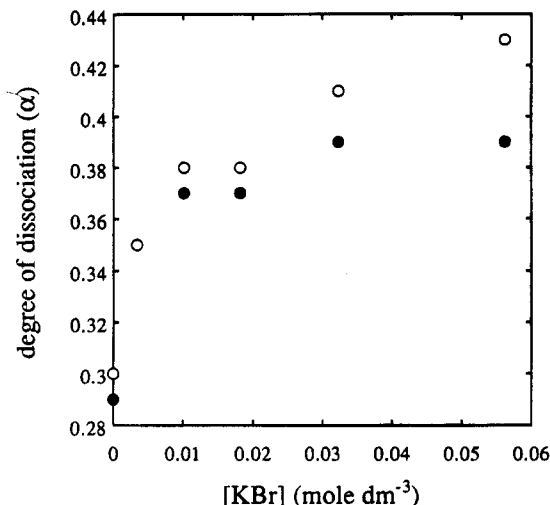


**Figure 11.** Calculated degrees of CTAB micellar dissociation,  $\alpha$ , as a function of KBr concentration. Values of  $\alpha$  are determined using both concentration (●) and activity (○) data.

The micellar surface charge density was obtained from the expression

$$\sigma_0 = eN_s\alpha/4\pi r^2 \quad (24)$$

where  $N_s$  is the micellar aggregation number,  $\alpha$  is the overall degree of surface dissociation, and  $r$  is the micellar radius. Micellar radii were calculated on the basis that

$$r = (3N_s V/4\pi)^{1/3} \quad (25)$$

where  $V$  is defined as the volume occupied by the hydrocarbon chain component of a surfactant monomer and was estimated from<sup>48</sup>

$$V = 27.4 + 26.9n_c \text{ (Å}^3\text{)} \quad (26)$$

where  $n_c$  is the number of carbon atoms per hydrocarbon chain. Micellar aggregation numbers were determined with empirical relationships obtained from static light scattering measurements of the CTAB/NaBr system.<sup>49</sup>

The background electrolyte concentration was calculated by neglecting possible contributions from charged self-assembled aggregates and dissociated micellar counterions; eq 13 was used.<sup>12</sup> Calculations were also performed by replacing concentrations with activities.

Degrees of micellar dissociation,  $\alpha$ , are given for the CTAB/KBr system in Figure 11. These  $\alpha$  values are those required to make the theoretical surface potential equal the experimental  $\psi_0$  value.  $\alpha$  values are not given beyond a concentration of *ca.* 0.06 M because the micelles become rodlike above this concentration. There is an increase in the calculated degree of micellar dissociation as the KBr concentration is increased.

Values for  $pK_{\text{diss}}$  calculated by using either  $n_0$  or  $A$  as a basis for  $\alpha$  are shown in Figure 12.  $pK_{\text{diss}}$  decreases with rising KBr concentration. The effect is less pronounced for values based upon activity data. The  $pK_{\text{diss}}$  values are of the expected order.<sup>36</sup> As for the planar interface, the variation of  $pK_{\text{diss}}$  with KBr concentration may be attributed to a changing interfacial microenvironment and/or the failure to take into account molecular protrusion (*inter alia*).

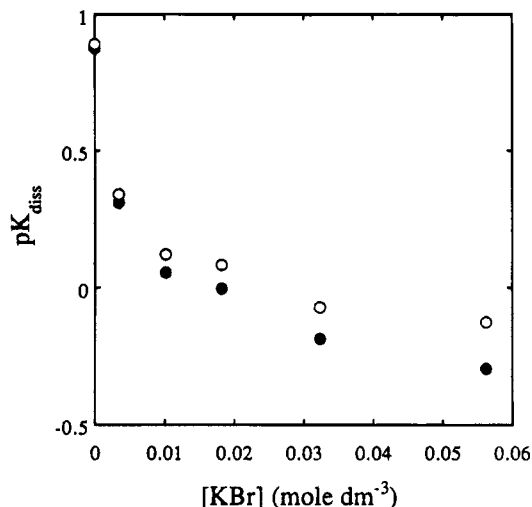


**Figure 12.** Calculated values of  $pK_{\text{diss}}$  for the CTAB micellar system with KBr concentration. Values for  $pK_{\text{diss}}$  are determined using both concentration (●) and activity (○) data.

Interestingly, there is a higher degree of CTAB dissociation calculated for spherical micelles than for planar adsorbed bilayers (*cf.* Figures 4 and 11). This may be a reflection that the geometry of the CTAB self-assembly aggregates spontaneously formed in water are spherical and rodlike, whereas at the solid interface the CTAB molecules are required to exist as a lamellar structure. Minimization of the free energy of the adsorbed CTAB lamellar system requires more quaternary ammonium headgroups to be electrically neutralized.

**Free Energy of Micellization.** If we assume that a surfactant monomer can be added to a micelle without altering its properties, then the chemical potential of the aggregate-based monomer,  $\mu_{\text{mic},\langle N_s \rangle}$ , may be given by<sup>50</sup>

$$\mu_{\text{mic},\langle N_s \rangle} = \mu_{\text{mic},\langle N_s \rangle}^\circ + ze\psi_0 + \mu_{\text{dipole}} \quad (27)$$

where  $\mu_{\text{mic},\langle N_s \rangle}^\circ$  is the standard chemical potential of the surfactant monomer in a micellar state,  $\mu_{\text{dipole}}$  is the chemical potential due to surface dipoles, and  $z$  is the valency of the surfactant amphiphile.

The chemical potential of a surfactant monomer in aqueous solution,  $\mu_{\text{aq}}$ , may be expressed as

$$\mu_{\text{aq}} = \mu_{\text{aq}}^\circ + kT \ln(a_{\text{aq}}) \quad (28)$$

where  $\mu_{\text{aq}}^\circ$  and  $a_{\text{aq}}$  are the standard chemical potential and the activity of the monomer in aqueous solution, respectively.

By assuming that a condition of equilibrium exists between surfactant monomers in the micellar and aqueous phases, eqs 27 and 28 may be combined to give

$$\psi_0 = \left( \frac{kT}{ze} \right) \ln(a_{\text{aq}}) + (\mu_{\text{aq}}^\circ - \mu_{\text{mic},\langle N_s \rangle}^\circ - \mu_{\text{dipole}})/ze \quad (29)$$

In practice, the critical micelle concentration may be used as an approximation to the monomer activity.<sup>50</sup> Provided that  $[(\mu_{\text{aq}}^\circ - \mu_{\text{mic},\langle N_s \rangle}^\circ - \mu_{\text{dipole}})/ze]$  remains relatively constant as a function of system ionic strength, then for

(48) Tanford, C. *The Hydrophobic Effect*; Wiley-Interscience: New York, 1973.

(49) Imae, T.; Kamiya, R.; Ikeda, S. *J. Colloid Interface Sci.* **1985**, *108*, 215.

(50) Healy, T. W.; Drummond, C. J.; Grieser, F.; Murray, B. S. *Langmuir* **1990**, *6*, 506.

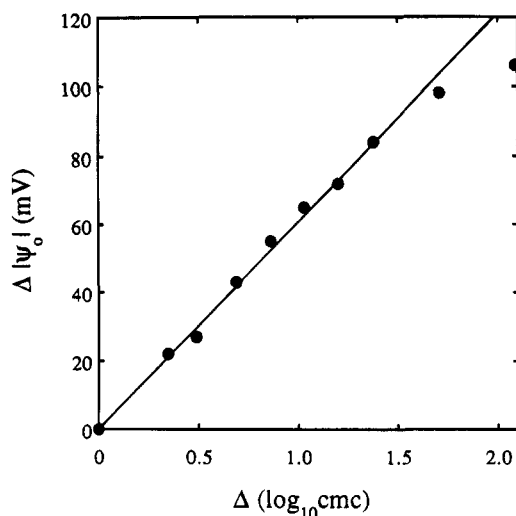


**Figure 13.** Values of  $\Delta|\psi_0|$  as a function of  $\Delta(\log \text{cmc})$  for the CTAB/KBr system. The line plot corresponds to a surface potential change of 60.55 mV per unit change in log cmc.

a charged univalent surfactant species at 32 °C

$$\frac{d|\psi_0|}{d \log(\text{cmc})} = 60.55 \text{ mV} \quad (30)$$

Figure 13 shows  $\Delta|\psi_0|$  versus  $\Delta(\log \text{cmc})$  for the CTAB/KBr system. The linear fit to the data corresponds to the predicted modulus change in surface potential of 60.55 mV per unit change in log cmc. It would appear then that it is a reasonable approximation to treat CTAB micelles in aqueous KBr solution as a bulk phase. The Nernstian behavior of the CTAB/KBr micellar system suggests that it may be reasonable to use the simple approach of Emerson and Holtzer<sup>51,52</sup> to calculate the hydrophobic contribution to the free energy of CTAB micellization. The approach of Emerson and Holtzer has been criticized on the basis that micelles cannot be treated as bulk phases.<sup>53–55</sup>

The standard free energy of micellization can be defined in many different ways.<sup>56</sup> In this work, the standard free energy of micellization,  $\Delta G^\circ_{\text{mic}}$ , was calculated as<sup>51,52</sup>

$$\Delta G^\circ_{\text{mic}} = RT \ln \text{cmc} \quad (31)$$

The thermodynamics of micelle formation can be thought of as a balance between a hydrophobic component,  $\Delta G_{\text{hc}}$ , due to the hydrocarbon portion of the surfactant monomer, and an electrostatic component,  $\Delta G_{\text{el}}$ , associated with the interaction between charged surfactant monomers and the micellar surface. The resulting relation is

$$\Delta G^\circ_{\text{mic}} = \Delta G_{\text{hc}} + \Delta G_{\text{el}} \quad (32)$$

For a Nernstian micellar system, the electrostatic free energy component can be expressed as

$$\Delta G_{\text{el}} = N_A e \psi_0 \quad (33)$$

Combination of eqs 31–33 provides the means by which the hydrophobic free energy component can be calculated

$$\Delta G_{\text{hc}} = RT \ln \text{cmc} - N_A e \psi_0 \quad (34)$$

Table 1 lists the calculated standard free energies of

**Table 1. Critical Micelle Concentration (cmc), Surface Potential ( $\psi_0$ ), Effective Interfacial Dielectric Constant ( $\epsilon_{\text{eff}}$ ), and Electrical ( $\Delta G^\circ_{\text{elec}}$ ) and Hydrophobic ( $\Delta G^\circ_{\text{hc}}$ ) Contributions to the Standard Free Energy of Micellization ( $\Delta G^\circ_{\text{mic}}$ ) for the CTAB/KBr System at 32 °C**

[KBr] (M)	cmc (M)	$\psi_0$ (mV)	$\epsilon_{\text{eff}}$	$\Delta G^\circ_{\text{mic}}$ (kJ/mol)	$\Delta G^\circ_{\text{elec}}$ (kJ/mol)	$\Delta G^\circ_{\text{hc}}$ (kJ/mol)
0	$9.55 \times 10^{-4}$	156	32	-17.5	15.1	-32.5
$3.40 \times 10^{-3}$	$3.63 \times 10^{-4}$	147	31	-19.9	14.2	-34.1
$1.02 \times 10^{-2}$	$1.55 \times 10^{-4}$	133	30	-22.0	12.8	-34.9
$1.82 \times 10^{-2}$	$1.02 \times 10^{-4}$	121	29	-23.1	11.7	-34.8
$3.23 \times 10^{-2}$	$6.87 \times 10^{-5}$	114	28	-24.1	11.0	-35.1
$5.62 \times 10^{-2}$	$4.70 \times 10^{-5}$	103	28	-25.0	9.9	-35.0
$1.00 \times 10^{-1}$	$3.16 \times 10^{-5}$	91	26	-26.0	8.8	-34.8
$1.97 \times 10^{-1}$	$2.00 \times 10^{-5}$	75	23	-27.2	7.2	-34.4
$3.16 \times 10^{-1}$	$1.45 \times 10^{-5}$	70	23	-28.0	6.8	-34.7
1.00	$6.59 \times 10^{-6}$	47	22	-30.0	4.5	-34.5

micellization and the electrostatic and hydrophobic components to  $\Delta G^\circ_{\text{mic}}$  for the CTAB/KBr system. With the exception of the case where there is no added KBr, values of  $\Delta G_{\text{hc}}$  remain relatively constant as a function of solution ionic strength. This demonstrated insensitivity to electrolyte concentration is in accordance with expectations.<sup>48,51,52,57,58</sup>

## Conclusions

For CTAB bilayers adsorbed on amorphous silica,  $\zeta$  potentials obtained from flat plate streaming potential and colloid electrophoretic mobility measurements are equivalent. With the colloid spheres and flat plates that have been investigated, providing the aqueous 1:1 electrolyte concentration is *ca.*  $10^{-3} \text{ mol dm}^{-3}$  or less, there is reasonable agreement between  $\psi_d$  values derived from AFM force curves and  $\zeta$  potentials obtained from the electrokinetic measurements. Above an aqueous 1:1 electrolyte concentration of  $10^{-3} \text{ mol dm}^{-3}$ ,  $\psi_d$  values derived from AFM force curves are significantly smaller than the  $\zeta$  potentials. Surface roughness is considered to be responsible for this discrepancy. The roughness problem, associated with AFM force curve analysis, is likely to manifest at much lower concentrations of multivalent counterions. In order to obtain quantitative  $\psi_d$  values from AFM force curves that have been obtained in relatively concentrated electrolyte solutions, either very smooth surfaces need to be employed or a procedure for dealing with the influence of random surface roughness needs to be developed.

The AFM force curves can show features that are indicative of adsorbed CTAB bilayers on silica.

Analysis of the electrostatic potentials in terms of conventional electrical double layer theory suggests that planar adsorbed CTAB layers on amorphous silica have a degree of dissociation ( $\alpha$ ) covered by the range 0.05–0.11, while spherical CTAB micelles have an  $\alpha$  value covered by the range 0.29–0.43. CTAB micelles behave as Nernstian objects in aqueous KBr solution with the surfactant monomer acting as the potential determining ion. This behavior suggests that a simple method can be employed to calculate the hydrophobic contribution to the standard free energy of micellization.

**Acknowledgment.** This work was begun while C.J.D. was the recipient of a Queen Elizabeth II Fellowship from the Australian Research Council (ARC). Funding of the Advanced Mineral Products Research Centre, a special Research Centre of the ARC, is gratefully acknowledged. We thank Professor T. W. Healy for helpful discussions.

LA940967E

(51) Emerson, M. F.; Holtzer, A. *J. Phys. Chem.* **1965**, *69*, 3718.

(52) Emerson, M. F.; Holtzer, A. *J. Phys. Chem.* **1967**, *71*, 1898.

(53) Mukerjee, P. *J. Phys. Chem.* **1969**, *73*, 2054.

(54) Stigter, D. *J. Colloid Interface Sci.* **1974**, *47*, 473.

(55) Gunnarsson, G.; Jonsson, B.; Wennerstrom, H. *J. Phys. Chem.* **1980**, *84*, 3114.

(56) Stenius, P.; Backlund, S.; Ekwall, P. *IUPAC Chem. Data Ser.* **1980**, *28*, 295.

(57) Evans, D. F.; Ninham, B. W. *J. Phys. Chem.* **1983**, *87*, 5025.

(58) Evans, D. F.; Ninham, B. W. *J. Phys. Chem.* **1984**, *88*, 6344.